Field-Induced Metal-Insulator Transition in the Pyrochlore Iridate $Nd_2Ir_2O_7$

Hiroaki Ishizuka[1]

Collaborators:

Timothy Hsieh[1,2], Leon Balents[1]

Experiments:

Z. Tian[3], Y. Kohama[3], T. Tomita[3], J. Ishikawa[3], K. Kindo[3], S. Nakatsuji[3]

[1] Kavli Institute for Theoretical Physics, University of California Santa Barbara

[2] Department of Physics, Massachusetts Institute of Technology

[3] Institute for Solid State Physics, the University of Tokyo

Aug. 2015 @ SO Matter, KITP, UCSB

Rare-Earth Moments in Pyrochlore Iridates

Does the rare-earth moments affect magnetic/transport properties?

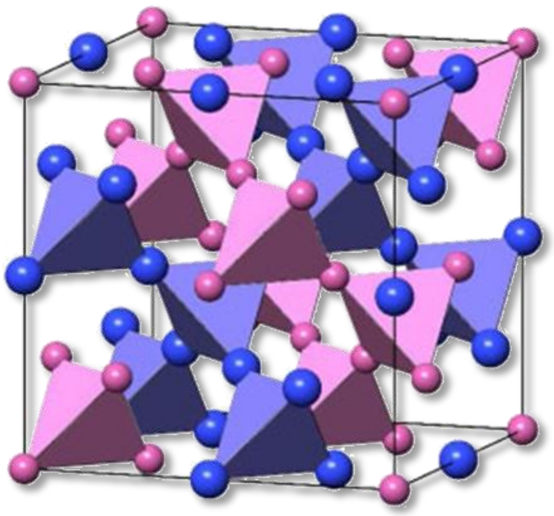

Iridium ions:

- Conduction electrons
- Moderately interacting
- Unique properties: quadratic band touching, Weyl semimetal, …

Rare-earth ions:

- Often form localized moment.
- Ignored in most of theoretical studies.

Rare-Earth Moments in Pyrochlore Iridates

Does the rare-earth moments affect magnetic/transport properties?

Ir pyrochlore ~ physics of Ir electrons?

- Band width *W* and Hubbard *U* ~ 1 eV; much larger than expected Kondo coupling J_K ~ 10 meV.
- MIT (mostly) takes place in the order of 100 K, and has weak dependence to *Ln* ions, magnetic or non-magnetic.

Matsuhira `12

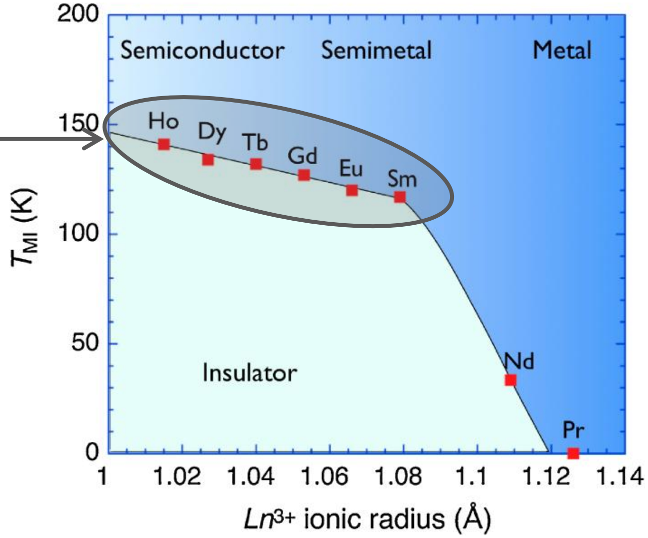

Rare-Earth Moments in Pyrochlore Iridates

Does the rare-earth moments affect magnetic/transport properties?

Ir pyrochlore ~ physics of Ir electrons?

- Band width W and Hubbard U ~ 1 eV; much larger than expected Kondo coupling J_K ~ 10 meV.
- MIT (mostly) takes place in the order of 100 K, and has weak dependence to Ln ions, magnetic or non-magnetic.

Matsuhira `12

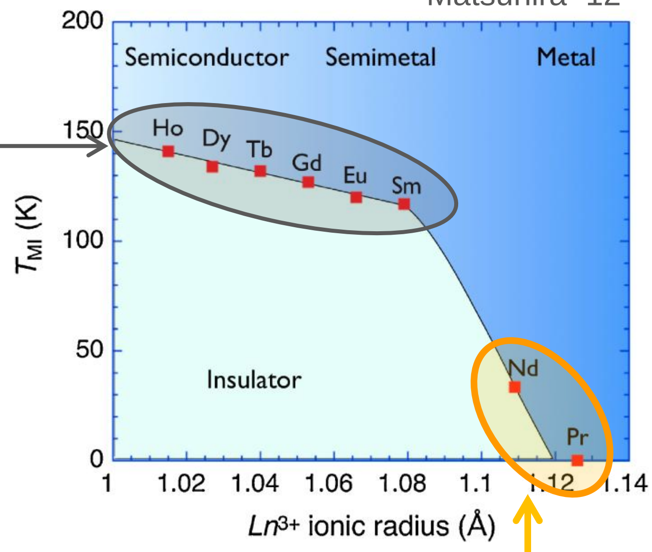

Kondo coupling may take important role if Ir electrons are at PM/AFM boundary.
→ $Nd_2Ir_2O_7$ may be one such example.

Field-Induced MIT in $Nd_2Ir_2O_7$

Zero-Field MIT in $Nd_2Ir_2O_7$

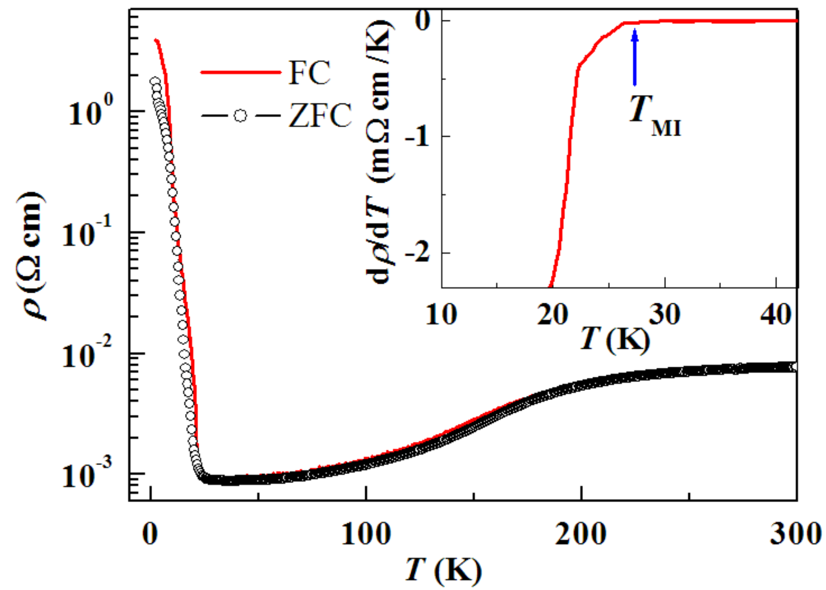

Resistivity Measurements:

1. Metal-insulator transition takes place at T_{MI}~30 K.
2. T_{MI} associated with the onset of AIAO order (mainly on Ir sites).

Tomiyasu `12

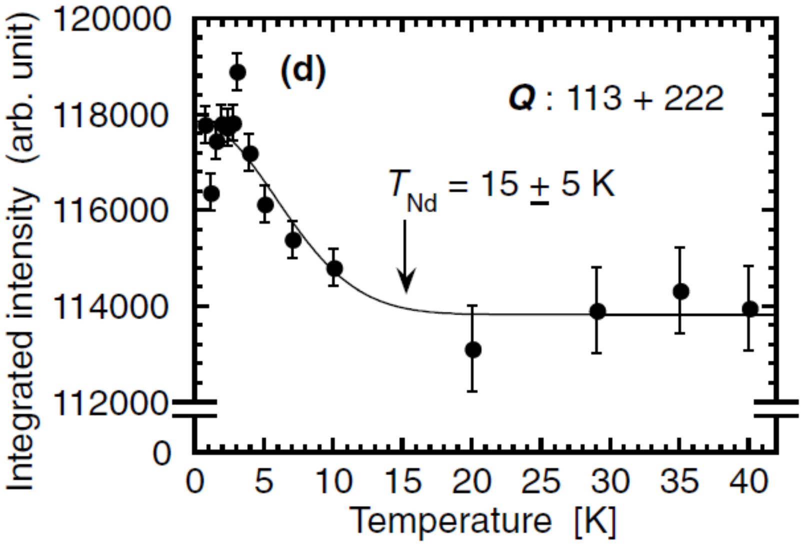

Neutron Diffraction:

1. Neutron being sensitive to Nd moments than the small Ir moments.
2. Onset of AIAO order on Nd sites (T_{Nd}~15 K) being lower than T_{MI} (~30K); ferromagnetic interactions between Nd moments?

Magnetization Process

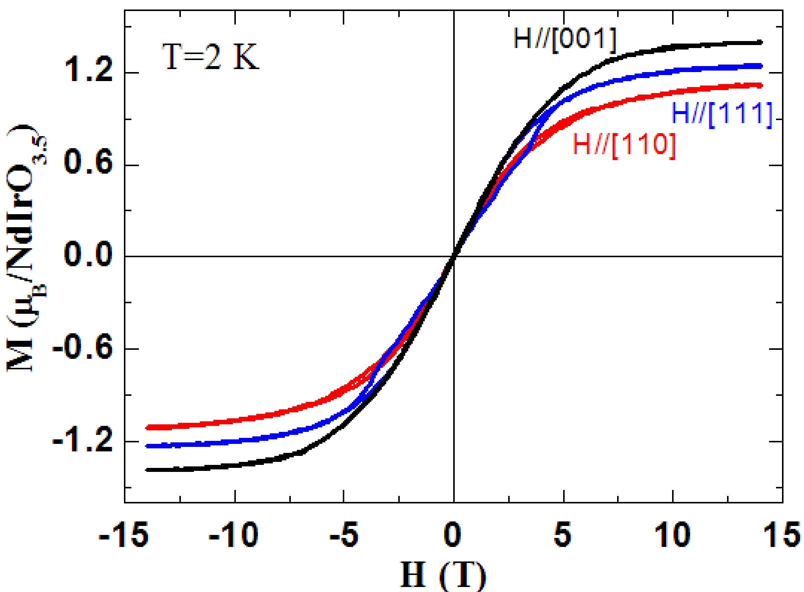

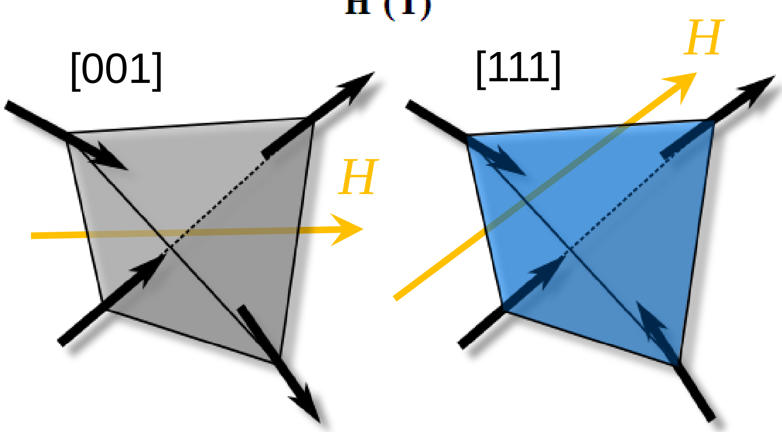

Magnetization Curve:

1. Saturation at magnetic field H~7 T.
2. Hysteresis for field along <111> while not for <100>.
3. Contribution mainly from Nd moments; the magnetization at saturation consistent with single-ion moment for Nd: $\mu_{Nd} \sim 2.4\mu_B$.
4. The result is also consistent with the expected small moments for Ir electrons $1/3 - 1/2\mu_B$.

Ising spins with local <111> axis (spin-ice):

1. AIAO for weak field.
2. 2-in 2-out for field along <100>, while 3-in 1-out for field along <111>.

Field-Induced Metal-Insulator Transition

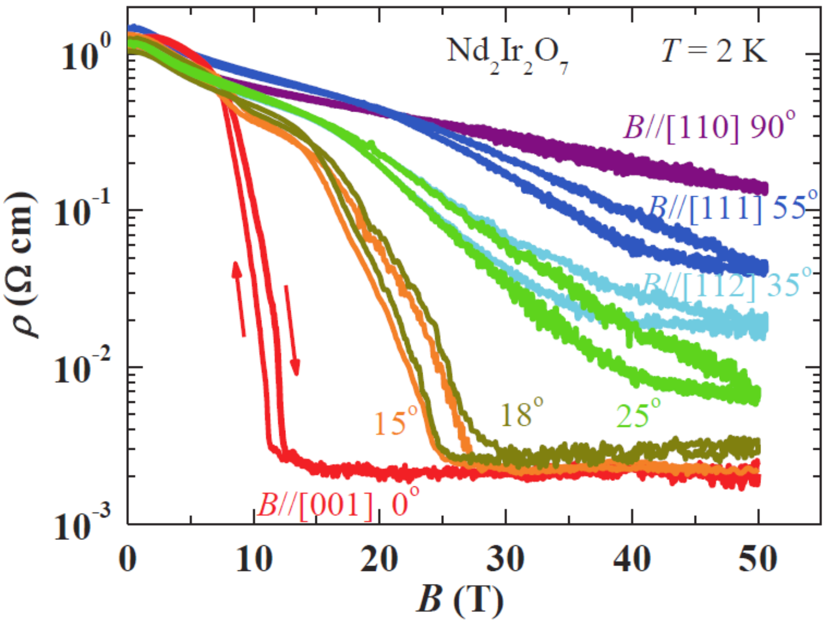

Metal-Insulator Transition

1. Sudden decrease of resistivity at B~10 T for field along [001].
2. Sharp metal-insulator transitions observed only for field close to [100] direction.
3. Hysteresis indicates 1st order transition.

Angle dependence of resistivity:

1. Large negative magneto-resistance observed only for field close to [001] direction.
2. Highly anisotropic behavior, unusual for cubic magnets.

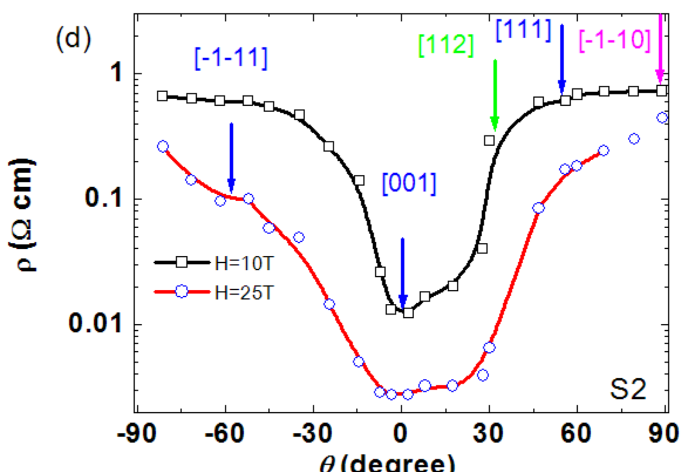

Similar results: K. Ueda *et al*., Phys. Rev. Lett. 115, 056402 (2015).

Field-Induced Metal-Insulator Transition

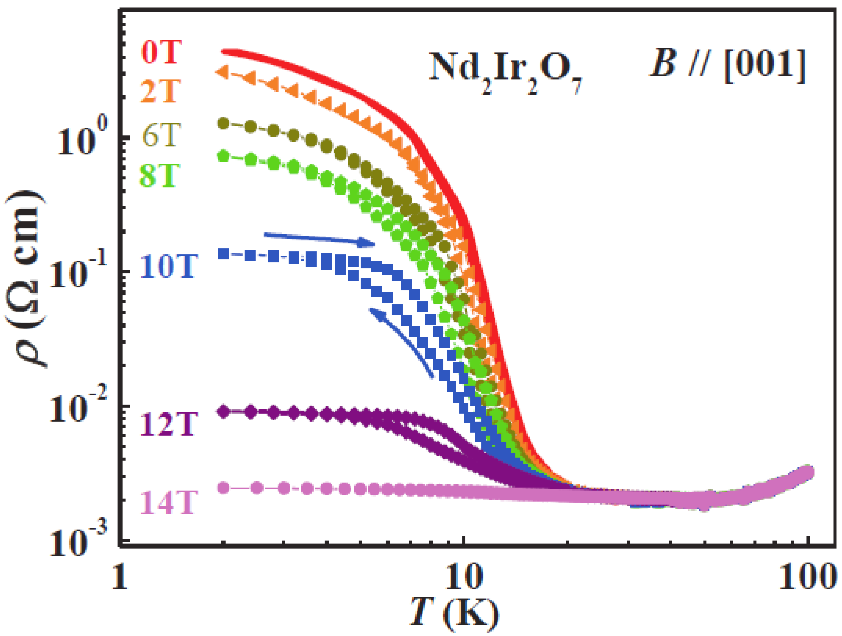

Suppression of MIT with magnetic field:

1. Metal-insulator transition suppressed by application of external magnetic field.
2. Hysteresis observed for MIT under strong magnetic field (no hysteresis for *B*=0); tricritical point at ~20 K and 2-6 T?
3. Weak temperature dependence of ρ in the high field (semi)metal phase.

Phase Diagram:

1. Ground state for low-field is a AIAO insulator.
2. High-field (semi)metal show very weak temperature dependence of ρ.

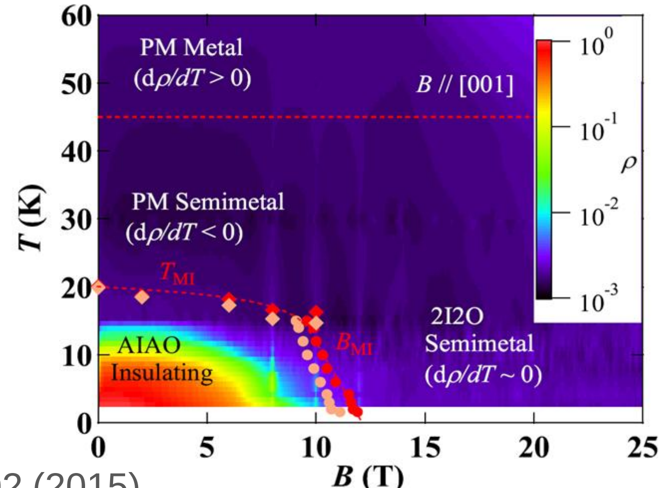

Similar results: K. Ueda *et al*., Phys. Rev. Lett. 115, 056402 (2015).

Effective Nd Spin Model

Rare-Earth Moments in $Ln_2Ir_2O_7$

Localized moments on *R* ions:

1. 4*f* electrons on *Ln* ions form localized moments, often with large *J*:

   J=4 for Pr^{3+} and J=9/2 for Nd^{3+}

2. Crystal field splits the degeneracy of moments.
3. May form pseudo-spins with multi-polar (quadrupolar/octupolar) moments with dipolar (magnetic) moments along the local *z* axis.

Interaction with Ir electrons:

1. 6 nearest Ir sites surrounding the *Ln* moments.
2. Kondo coupling between Ir electrons and *R* moments may have unconventional form due to the multi-polar nature of *R* moments.
3. Mediates RKKY interaction between Nd moments.

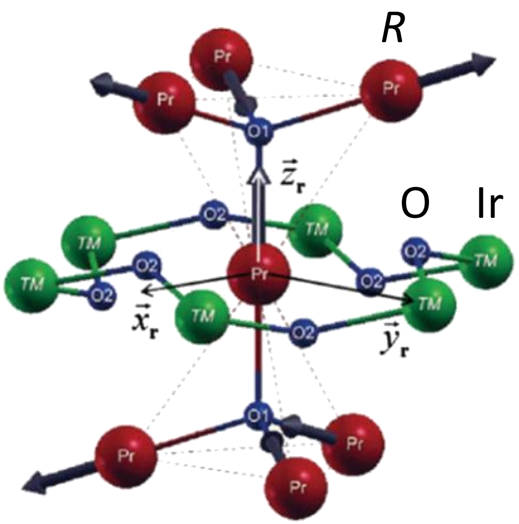

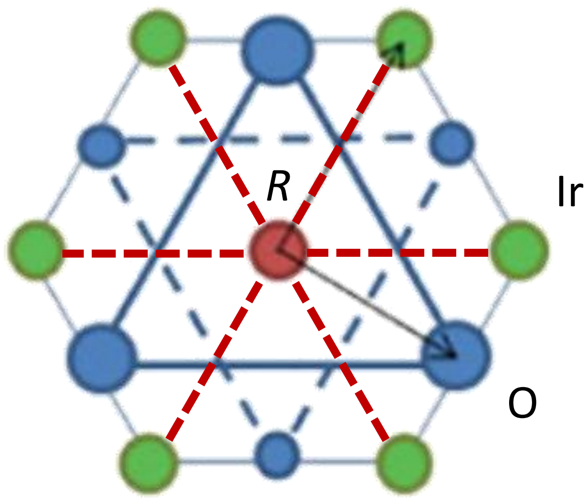

S. Onoda `10

Doublets of Nd Moments

1. Due to the highly anisotropic crystal field, the J=9/2 Nd moments split into 5 Kramers doublets.
2. The resultant ground state doublet is a dipolar-octupolar doublet. (Huang `14)
3. Investigated by neutron scattering measurement.

Table 1. Calculated CEF parameters, eigenenergies and eigenstates for Nd^{3+} (J = 9/2). Ten coefficients with respect to $|J_z>$ are given for each eigenstates.

CEF parameters [meV]					
B_2^0	B_4^0	B_4^3	B_6^0	B_6^3	B_6^6
-0.28(0)	$-0.95(9)\times10^{-2}$	-0.33(9)	$-0.44(3)\times10^{-3}$	$0.17(7)\times10^{-2}$	$-0.45(7)\times10^{-2}$

eigenenergies [meV] and eigenstates										
E_i	| -9/2>	| -7/2>	| -5/2>	| -3/2>	| -1/2>	| 1/2>	| 3/2>	| 5/2>	| 7/2>	| 9/2>
123	0	0	0.375	0	0	0.533	0	0	-0.758	0
123	0	-0.758	0	0	-0.533	0	0	0.375	0	0
57	0.135	0	0	-0.289	0	0	-0.772	0	0	0.550
57	0.550	0	0	0.772	0	0	-0.289	0	0	-0.135
42	0	0	-0.439	0	0	-0.617	0	0	-0.653	0
42	0	0.653	0	0	-0.617	0	0	0.439	0	0
26	0	0	0.816	0	0	-0.578	0	0	-0.003	0
26	0	0.003	0	0	0.578	0	0	0.816	0	0
0	-0.057	0	0	-0.286	0	0	-0.489	0	0	-0.822
0	-0.822	0	0	0.489	0	0	-0.286	0	0	0.057

Tomiyasu `11

Model: Effective spin model for Nd moments

$$\mathcal{H}_{Nd}^{(\mathrm{eff})} = \sum_{\langle i,j \rangle} J_z \tau_i^z \tau_j^z + J_y \tau_i^y \tau_j^y + J_x \tau_i^x \tau_j^x + J_{xz}(\tau_i^x \tau_j^z + \tau_i^z \tau_j^x) - A_H \sum_i \tau_i^z - g \sum_i \tau_i^z (\boldsymbol{a}_i \cdot \boldsymbol{h})$$

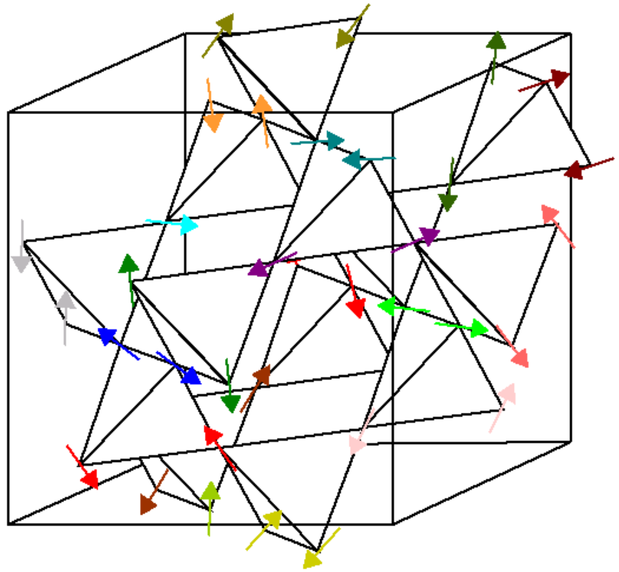

1. Spin model on a pyrochlore lattice with nearest-neighbor interactions.
2. The moments are dipolar-octupolar moments.
3. Interactions and Zeeman coupling terms allowed by symmetry.

Parameters:
J_x=J_y=-0.0001, J_{xz}=0.0001, g=0.001

Magnetization Process

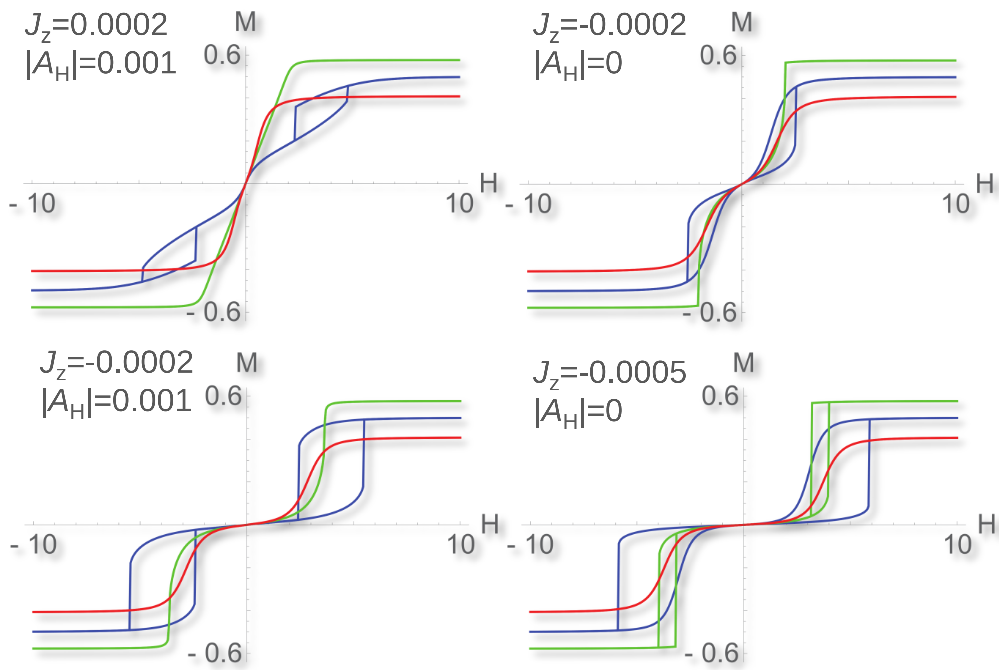

1. Magnetization process of Nd moments coupled to AIAO field from iridium ions (A_H) with external field applied along <100> (green), <110> (red), <111> (blue).
2. A_H is flipped at H=0 to mimic the behavior of order parameter.
3. Ferromagnetic J_z reproduces hysteresis for <111> at h~0, while other terms (J_x, J_y, …) contributes to smooth out the curves.

Kondo Lattice Model

Model: Ir Electrons + Nd Moments

Iridium Electrons: Tight-binding model for J_{eff}=1/2 bands with 2nd neighbor hopping + onsite Hubbard *U*. (Witczak-Krempa `13)

Kondo Coupling between Ir and Nd ions:

$$\mathcal{H}_K = J_K \sum_{ij} \Lambda_{ij}^{\mu\nu} S_i^{\mu} \tau_j^{\nu} \qquad \mathcal{H}_h^{\text{Nd}} = -\gamma \sum_i (\mathbf{h} \cdot \boldsymbol{a}_i) \tau_i^z$$

$$\Lambda_{ij}^{\mu\nu} = \begin{cases} G_1^x\, \boldsymbol{a}_j \cdot \hat{\boldsymbol{e}}_\mu + G_2^x\, \boldsymbol{a}_j \bar{\times} (\boldsymbol{d}_{ij} \bar{\times} \boldsymbol{d}_{ij}) \cdot \hat{\boldsymbol{e}}_\mu & (\nu = x) \\ G^y\, \boldsymbol{a}_j \times (\boldsymbol{d}_{ij} \bar{\times} \boldsymbol{d}_{ij}) \cdot \hat{\boldsymbol{e}}_\mu & (\nu = y) \\ G_1^z\, \boldsymbol{a}_j \cdot \hat{\boldsymbol{e}}_a + G_2^z\, \boldsymbol{a}_j \bar{\times} (\boldsymbol{d}_{ij} \bar{\times} \boldsymbol{d}_{ij}) \cdot \hat{\boldsymbol{e}}_\mu & (\nu = z) \end{cases}$$

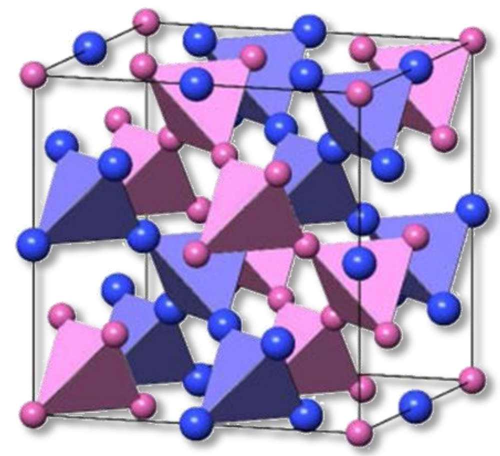

1. We consider effective Hamiltonian taking into account of the lowest energy doublets for Nd ions (dipolar-octupolar doublets).

   (Huang `14)

2. We only consider coupling of Nd moments to Ir electrons (Kondo couplings) due to the highly localized nature of Nd 4*f* electrons.

3. We consider all types of couplings allowed by symmetry.

Mean Field Theory

$$\mathcal{H}_U \simeq U\sum_{i\sigma}\langle c^\dagger_{i\sigma}c_{i\sigma}\rangle c^\dagger_{i\bar\sigma}c_{i\bar\sigma} - \langle c^\dagger_{i\sigma}c_{i\bar\sigma}\rangle c^\dagger_{i\bar\sigma}c_{i\sigma} - U\sum_{i}\langle c^\dagger_{i\uparrow}c_{i\uparrow}\rangle\langle c^\dagger_{i\downarrow}c_{i\downarrow}\rangle - \langle c^\dagger_{i\uparrow}c_{i\downarrow}\rangle\langle c^\dagger_{i\downarrow}c_{i\uparrow}\rangle$$

$$\begin{aligned}\mathcal{H}_K &\simeq J_K\sum_{ij}\Lambda^{\mu\nu}_{ij}\left[\langle S^\mu_i\rangle\tau^\nu_j + S^\mu_i\langle\tau^\nu_j\rangle - \langle S^\mu_i\rangle\langle\tau^\nu_j\rangle\right] \\ &= J_K\sum_{ij}\Lambda^{\mu\nu}_{ij}S^\mu_i\,\langle\tau^\nu_j\rangle.\end{aligned}$$

1. To take into account of the spacial correlation, we consider eight site cluster with four spins and four half-filled electron sites.
2. Mean-field expansion using unrestricted Hartree-Fock method for Ir electrons and mean-field treatment for localized Nd moments.

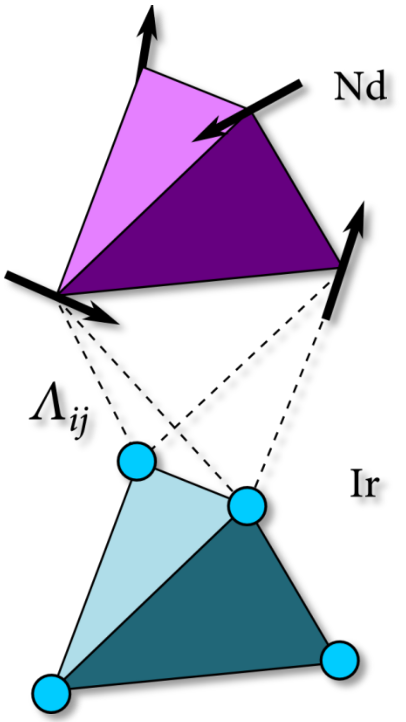

Fermion-Mediated Interactions

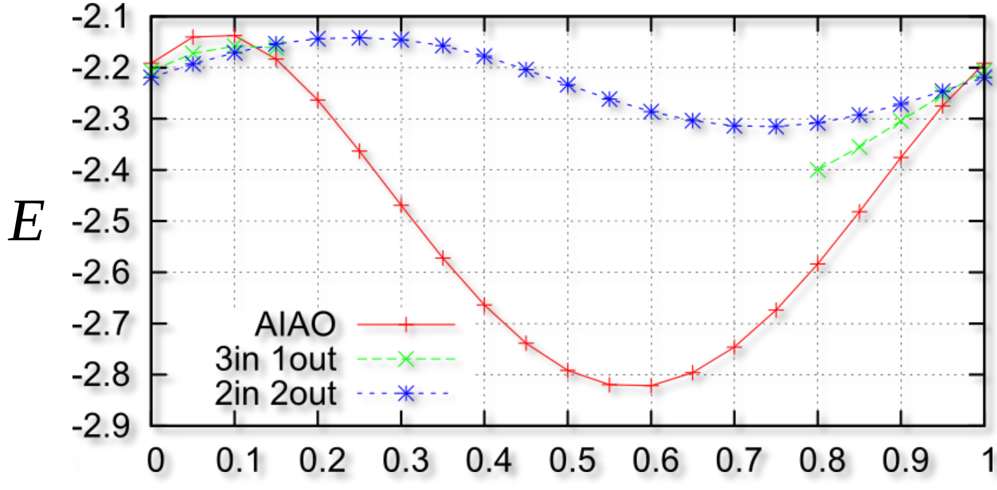

$$\theta = \arctan(G_2^z / G_1^z)$$

1. We first look for the appropriate set of Kondo couplings with ferromagnetic nearest-neighbor interaction along *z* axis.
2. Ground state energy for (meta-)stable all-in all-out, two-in two-out, and three-in one-out states by mean-field calculation with different ratio of G_1^z and G_2^z.
3. All-in all-out become the ground state when G_2^z is dominant while two-in two-out is favored for G_1^z. This implies the nearest-neighbor interaction to be <u>ferromagnetic when G_1^z is dominant while antiferromagnetic for G_2^z</u>.
4. In the following, we consider $|G_1^z| >> |G_2^z|$.

Enhanced AIAO Order by Kondo Coupling

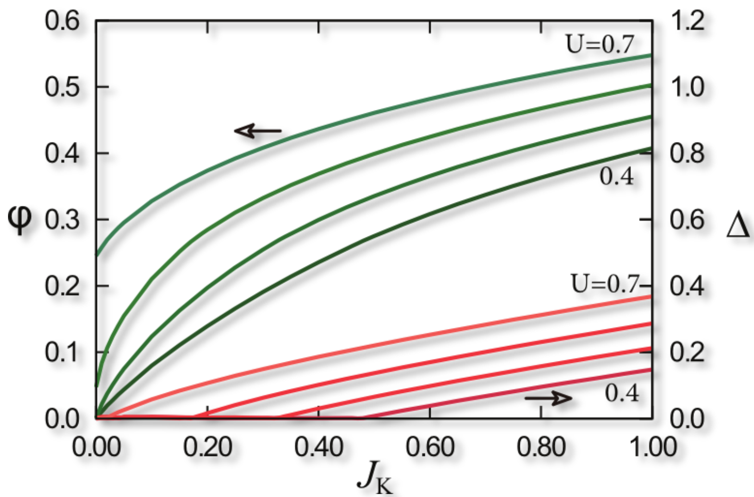

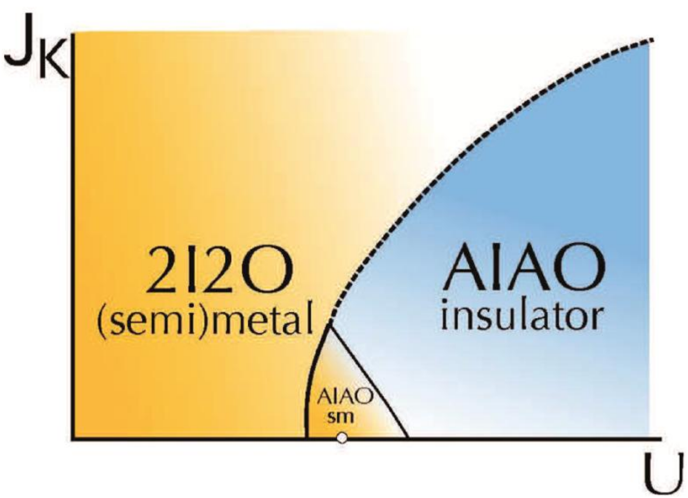

1. AIAO order parameter for Ir electrons (green) and the charge gap (red).

2. AIAO order being enhanced by the Kondo coupling, and AIAO order appears in weak U region where AIAO does not exists for J_K=0.

3. The charge gap induced by the Kondo coupling.

4. (below) Schematic phase diagram with J_K and U.

Parameters:

t_{oxy}=1, t_σ=-1.1 , t_π=-(2/3) t_σ, $t'_{\pi,\sigma}$ =0.02 $t_{\pi,\sigma}$

G_1^x=0.0, G_2^x=0.006, G^y=0.01,
G_1^z=-0.06, G_2^z=-0.02

Magnetization Process

Parameters:

t_{oxy}=1, t_σ=-1.1 , t_π=-(2/3) t_σ, $t'_{\pi,\sigma}$ =0.02 $t_{\pi,\sigma}$

G_1^x=0.0, G_2^x=0.006, G^y=0.01,
G_1^z=-0.06, G_2^z=-0.02, γ = 5.0

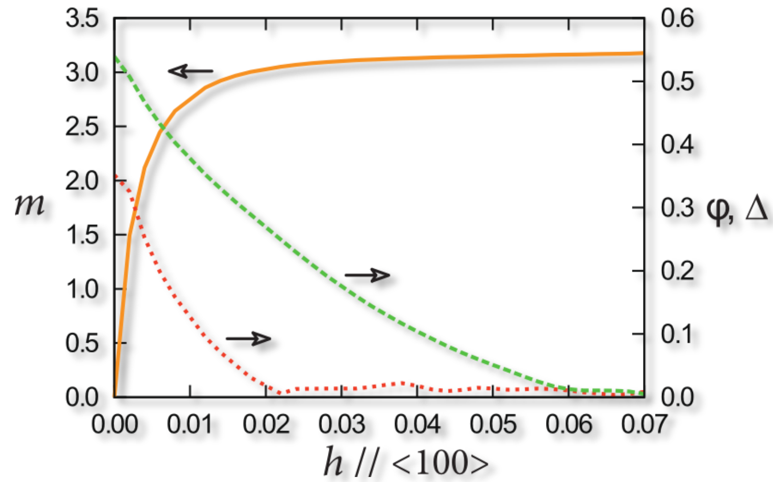

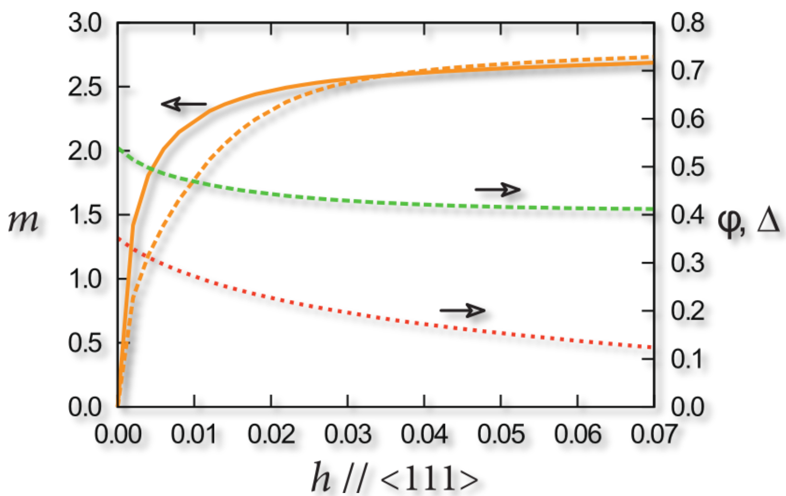

1. AIAO order parameter for Ir electrons (green) , charge gap (red), and net magnetization along the external field (orange).

2. A metal-insulator transition occurs when the field is applied along <100> direction, while no transition for <111>. They are highly anisotropic.

3. The magnetization curve show hysteresis for field along <111>. This is due to the lifting of the degeneracy of two AIAO ground states at *h*=0.

4. Very small critical *h* (~0.01) compared to *U* (~1), due to large γ.

Zhaoming Tian *et al*., submitted.

Summary

1. We studied magnetization process and metal-insulator transition in $Nd_2Ir_2O_7$.
2. We found a field-induced metal-insulator transition.
3. The MIT is highly anisotropic, unusual for cubic magnets.
4. The form of magnetization curves being strongly affected by the effective interaction between Nd localized moments.
5. The Kondo coupling between Nd moments and Ir electrons has significant effects over magnetic and electronic property of the material.
   - ✓ Very low h_c compared to Hubbard U.
   - ✓ Highly anisotropic MIT with applied magnetic field.
6. Anisotropic hysteresis in magnetization curve is a consequence of AIAO ground state.